Earth, Planets and Space

FULL PAPER

Open Access

Non-monotonic growth and motion of the South Atlantic Anomaly

Hagay Amit[1*], Filipe Terra-Nova[2], Maxime Lézin[1] and Ricardo I. Trindade[2]

Abstract

The South Atlantic Anomaly (SAA) is a region at Earth's surface where the intensity of the magnetic field is particularly low. Accurate characterization of the SAA is important for both fundamental understanding of core dynamics and the geodynamo as well as societal issues such as the erosion of instruments at surface observatories and onboard spacecrafts. Here, we propose new measures to better characterize the SAA area and center, accounting for surface intensity changes outside the SAA region and shape anisotropy. Applying our characterization to a geomagnetic field model covering the historical era, we find that the SAA area and center are more time dependent, including episodes of steady area, eastward drift and rapid southward drift. We interpret these special events in terms of the secular variation of relevant large-scale geomagnetic flux patches on the core–mantle boundary. Our characterization may be used as a constraint on Earth-like numerical dynamo models.

Keywords: Geomagnetic field, Secular variation, South Atlantic Anomaly, Core–mantle boundary

Introduction

The South Atlantic Anomaly (SAA) is a region at Earth's surface where the intensity of the magnetic field is particularly low. This leads to penetration of solar energetic particles deep into Earth's atmosphere, posing severe problems for airplanes and ships positioning systems as well as spacecraft electronic systems (Konradi et al. 1994; Deme et al. 1999; Heirtzler 2002; Lean 2005; Auvergne et al. 2009; Domingos et al. 2017). Understanding the past and present locations and mobility as well as the future trajectory of the SAA is both a fundamental scientific challenge—it involves understanding the working of the geodynamo and the impact of core–mantle coupling on core dynamics, as well as an important societal issue—it has major consequences for the operation and protection of surface instruments and spacecrafts, from global positioning systems to the Hubble Space Telescope, which cannot obtain observations over the SAA region.

The current location of the SAA center in Brazil is related to the location of reversed geomagnetic flux patches (RFPs) at the core–mantle boundary (CMB) (Bloxham et al. 1989; Olson and Amit 2006) though this relation is not trivial (Terra-Nova et al. 2017). It is under debate whether the current SAA location represents a persistent boundary-driven feature of Earth's magnetic field or it is chaotically variable. Based on a data assimilation scheme, Aubert (2015) predicted that the SAA will drift in the near future to the Pacific, i.e. it may suggest a transient feature of the geodynamo. However, the centennial forecast of Aubert (2015) is too short to determine with confidence the long-term behavior of the SAA. In contrast, based on archeological materials, it was argued that the SAA has influenced the surface geomagnetic field for several millennia in Africa (Tarduno et al. 2015; Hare et al. 2018) and South America (Trindade et al. 2018; Hartmann et al. 2019). Tarduno et al. (2015) used such local intensity and directional timeseries, together with observation of a Large Low Shear Velocity Province (LLSVP) in the lowermost mantle below Africa coincident with a historical African RFP on the CMB (e.g. Jackson et al. 2000), to propose that core flux expulsion occurred preferentially

*Correspondence: Hagay.Amit@univ-nantes.fr
[1] CNRS UMR 6112, Université de Nantes, Laboratoire de Planétologie et de Géodynamique, 2 rue de la Houssinière, Nantes 44000, France
Full list of author information is available at the end of the article

at the edge of the LLSVP. In this model, RFPs form stochastically at the LLSVP edge and are then advected westward. A prediction of this model was that a low intensity feature observed in the African archeomagnetic record would be observed later in South America (Tarduno 2018). This scenario is in agreement with subsequent archeomagnetic intensity timeseries from South America and is supported by some synthetic kinematic scenarios (Trindade et al. 2018). The time lag between the Africa and South America surface minima, however, requires frequent expulsion of multiple RFPs (Trindade et al. 2018).

Because of the limited amounts of archeomagnetic data from the southern hemisphere, care must be taken in the interpretation of any archeomagnetic field models applied to the SAA region. Nevertheless, some interesting results have been reported that may guide further data collection. For example, some archeomagnetic field models exhibit persistent surface intensity minimum in the South Atlantic (Brown et al. 2018; Hellio and Gillet 2018; Panovska et al. 2019). Campuzano et al. (2019) found evidence that the SAA has been expanding and westward drifting since 1400.

Heterogeneous CMB conditions may affect the morphologies of outer core convection and the induced geomagnetic field. Numerical dynamo simulations with imposed tomographic outer boundary heat flux have been widely applied to explore geodynamo features, most commonly preferred locations of intense geomagnetic flux patches on the CMB (Gubbins et al. 2007; Aubert et al. 2008; Amit et al. 2015). Terra-Nova et al. (2019) applied such models to show that the longitude of the SAA center may be mantle controlled; However, recovering its relatively large latitude remains a challenge.

Geomagnetic field models spanning the historical era (e.g. Jackson et al. 2000) and more recent modern periods (e.g. Finlay et al. 2010) may provide reliably the location, mobility and area of the SAA. However, previous SAA characterizations which are useful in the context of space safety, can be improved and designed to be more useful for exploring its core dynamical origin. In this paper, we will show that SAA area estimates based on a fixed threshold (De Santis et al. 2013; Pavón-Carrasco and De Santis 2016; Campuzano et al. 2019) are affected by global variations and as such might not represent adequately regional morphological changes of the geomagnetic field. Furthermore, SAA center estimates based on surface minimum positions (e.g. Terra-Nova et al. 2017) do not take into account anisotropic SAA shape. In order to better understand the kinematic origin of the SAA and constrain numerical dynamos (Terra-Nova et al. 2019), a more appropriate characterization of the SAA in terms of its area and center is required.

Previous studies characterized the SAA at altitudes of ~ 800 km above Earth's surface, corresponding to low-Earth orbits of satellites (Casadio and Arino 2011; Schaefer et al. 2016; Anderson et al. 2018). Here, we characterize the SAA at Earth's surface where geomagnetic observations have been continuously acquired since the advent of intensity measurement (Jackson et al. 2000). We then explore the outer core kinematic origin of the SAA temporal variability.

The paper is outlined as follows. In Sect. "Method" we introduce and justify our new measures of the SAA area and center. The results for this SAA characterization are presented in Sect. "Secular variation of the area and center of the South Atlantic Anomaly" and the kinematic interpretations in terms of temporal evolution of relevant flux patches on the CMB are given in Sect. "Outer core kinematic interpretation". We conclude our main findings in Sect. "Conclusions".

Method

We compare the characterization of the SAA based on previous studies vs. our proposed measures. This characterization includes both the area and the coordinates of the SAA center.

Previous studies defined the SAA area as that where the geomagnetic field intensity $|\vec{B}|$ at Earth's surface is lower than 32,000 nT (De Santis et al. 2013; Pavón-Carrasco and De Santis 2016):

$$|\vec{B}| < 32,000\,\mathrm{nT}. \tag{1}$$

From hereafter we term the area based on (1) as *S0*. This definition is practical for space safety purposes. However, from a more fundamental point of view, (1) is affected not only by regional spatio-temporal field variations, but also by global changes. Fig. 1 illustrates this point. Under a hypothetical scenario of entire field magnitude decrease with no pattern change, a fixed critical threshold (such as 32,000 nT) for the SAA would suggest that its area increases despite no regional variation.

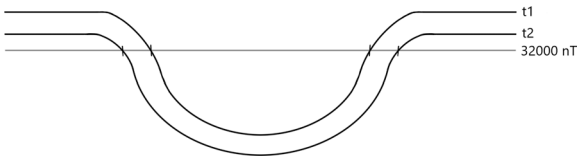

Fig. 1 Schematic illustration of a cross section of the surface field intensity under a global decrease in field intensity from time *t1* to time *t2*. In this scenario, the apparent SAA area based on *S0* (1) increases

To overcome this possible problem, alternatively, we factor the critical intensity value by the instantaneous mean surface intensity outside the SAA normalized by its value at the middle of the investigated period, which we term $F_{\rm out}$:

$$F_{\rm out} = \frac{\int_0^{2\pi}\int_0^{\pi/2}|\vec{B}|(t)\sin\theta d\theta d\phi + \int_{\pi/2}^{3\pi/2}\int_{\pi/2}^{\pi}|\vec{B}|(t)\sin\theta d\theta d\phi}{\int_0^{2\pi}\int_0^{\pi/2}|\vec{B}|(1930)\sin\theta d\theta d\phi + \int_{\pi/2}^{3\pi/2}\int_{\pi/2}^{\pi}|\vec{B}|(1930)\sin\theta d\theta d\phi}. \quad (2)$$

For this purpose, for the area outside the SAA, we consider the northern hemisphere plus the Pacific (i.e. between 90°E and 270°E) southern hemisphere:

$$|\vec{B}| < 32000F_{\rm out}\,{\rm nT}, \quad (3)$$

where ϕ and θ are longitude and co-latitude, respectively. Similar planetary-scale averages were recently invoked to quantify the Pacific/Atlantic geomagnetic SV dichotomy (Dumberry and More 2020) or the northern/southern differences in the SV-induced neutral density of the thermosphere (Cnossen and Maute 2020). Note that while the choice of the mid-term year 1930 in the denominator of (3) is completely arbitrary, this has no consequence on the resulting rate of change of the SAA area. From hereafter, we term the area based on (3) as $S1$. With this definition, the critical value varies with the mean surface intensity away from the SAA. As such, it captures the regional variation of the SAA area, independent of the change in the field magnitude elsewhere.

Next, previous studies tracked the SAA center based on the point of minimum field intensity, both at Earth's surface (Hartmann and Pacca 2009; Finlay et al. 2010; Aubert 2015; Terra-Nova et al. 2017, 2019) and at higher altitudes (Anderson et al. 2018). Following Terra-Nova et al. (2017), we reproduce this result by first searching for the grid point with lowest intensity and then applying second-order polynomial interpolations using two neighboring points in each direction to resolve off-grid values. From hereafter, we term these coordinates as Min. Note that this definition of a center is advantageous in some useful applications, e.g. in determining the maximum cutoff of radiation vs. duration at a certain radiation level for a spacecraft traversing the SAA. In the context of a core origin, if the shape of the SAA is significantly anisotropic, the minimum point might not well represent the center of the structure (for an illustration see Fig. 2).

Alternatively, centers of mass were invoked to identify and track centers of intense flux patches on the CMB in numerical dynamos (Amit et al. 2010) and geomagnetic field models (Amit et al. 2011). Centers of mass were also used to identify the SAA at $\sim$ 800 km altitude (Casadio and Arino 2011; Schaefer et al. 2016). Here, we calculate centers of mass to determine the longitude and co-latitude of the SAA center, $\phi_{\rm cm}$ and $\theta_{\rm cm}$, respectively, at Earth's surface:

$$\phi_{\rm cm} = \frac{\sum_S \phi_i w_i}{\sum_S w_i}, \quad (4)$$

$$\theta_{\rm cm} = \frac{\sum_S \theta_i w_i}{\sum_S w_i}. \quad (5)$$

The summations in (4)–(5) are over the SAA area, either $S0$ or $S1$, which we term CM0 and CM1, respectively. The weight w is given by the inverse of the intensity

$$w_i = \frac{1}{|\vec{B}_i|}. \quad (6)$$

Determining the center of the SAA based on the center of mass of its area well represents the center even if its shape is significantly anisotropic.

Finally, we monitor the time dependence of the value of minimum surface intensity $|\vec{B}|_{\rm min}$. In addition, we define a relative minimum surface intensity $|\vec{B}|^{\rm rel}_{\rm min}$ with respect to the instantaneous field intensity outside the SAA. Similar to (3), we calculate $|\vec{B}|^{\rm rel}_{\rm min}$ using $F_{\rm out}$ (2) as follows:

$$|\vec{B}|^{\rm rel}_{\rm min} = |\vec{B}|_{\rm min}/F_{\rm out}. \quad (7)$$

Both areas $S0$ and $S1$ were calculated using a simple trapezoid numerical scheme. Tests of the dependence of the results on the grid size show very weak sensitivity and fast convergence with increasing resolution. For all calculations we used a $1^\circ \times 1^\circ$ grid in longitude and co-latitude. With this grid size, the computed properties (i.e. the area and coordinates of the center) practically reach asymptotic values with decreasing grid size.

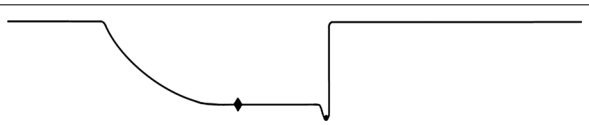

Fig. 2 Schematic illustration of a cross section of the surface field intensity with an anisotropic configuration. The SAA center based on the minimum (Min, denoted by a point) does not represent well the center of the anomaly. The center of mass method (CM0 or CM1) gives an adequate center denoted by a diamond

Secular variation of the area and center of the South Atlantic Anomaly

We used the COV-OBS.x1 time-dependent geomagnetic field model (Gillet et al. 2015) for the period 1840–2020. This model is advantageous for two main reasons. First, it covers the entire historical period, allowing to avoid different field models constructed based on different methods for different epochs (as was previously done in the SAA context by, e.g. Pavón-Carrasco and De Santis 2016; Terra-Nova et al. 2017). Second, COV-OBS.x1 is an ensemble of 100 realizations generated by a stochastic process from estimated mean and covariance of the model coefficients. This approach accounts for the lower precision of geomagnetic data at earlier times and for the uneven geographical distribution of geomagnetic data (Gillet et al. 2013). The 100 realizations represent 100 possible combinations of Gauss coefficients with comparable misfit to the observations.

Figure 3 shows the intensity of the geomagnetic field at Earth's surface for four snapshots. Before 1930 (Fig. 3, top), the SAA area based on *S*0 (green dashed contour) was smaller than the area based on *S*1 (purple dashed contour); whereas after 1930 (Fig. 3, bottom), the area based on *S*0 was larger. This is trivially expected from the definition of *S*1 (3). However, the visible differences between *S*0 and *S*1 in Fig. 3 provide testimony to the contribution of the temporal variability of the surface intensity outside the SAA to the apparent increase of the SAA area. The centers of the SAA based on Min, CM0 and CM1 are very similar at early snapshots when the SAA area was rather isotropic. However, towards present day the shape of the SAA became more complex with thin branches extending to equatorial east Pacific and South Africa. This anisotropic shape produced significantly different centers for Min, CM0 and CM1.

Figure 4 quantifies the characterization of the SAA over the entire period 1840–2020. Overall, the minimum intensity (purple in Fig. 4a) has been monotonically decreasing, except for the period $\sim$ 1890–1920 when it deviated from the overall linear trend. The relative minimum intensity (7) even shows a mild increase in that period (turquoise in Fig. 4a). The increase of the SAA area (Fig. 4b) based on *S*0 (yellow) is quite monotonic. Less so is the evolution of *S*1 (turquoise), including a period between $\sim$ 1890 and 1940 (see dashed vertical lines in Fig. 4) when *S*1 was flat. The longitude of the SAA center (Fig. 4c) based on Min (purple) has been monotonically decreasing, corresponding to a westward drift. In contrast, the SAA center longitudes based on CM0 (yellow) and CM1 (turquoise) are more variable. Most of the time, the SAA based on these two models have also been drifting westward, but significantly slower. Moreover, between $\sim$ 1940 and 1980, CM0 and CM1 have been drifting eastward. The latitude of the SAA center (Fig. 4d) has been decreasing, corresponding to a southward drift. According to Min (purple), this southward drift has been decaying with time. The CM0 (yellow) and CM1 (turquoise) latitudes were fairly flat before $\sim$ 1900 and after $\sim$ 1980; whereas in between these two epochs, both models exhibited a rapid southward drift. Overall, the SAA area and motion based on the previously proposed models *S*0 and Min are rather monotonic; whereas

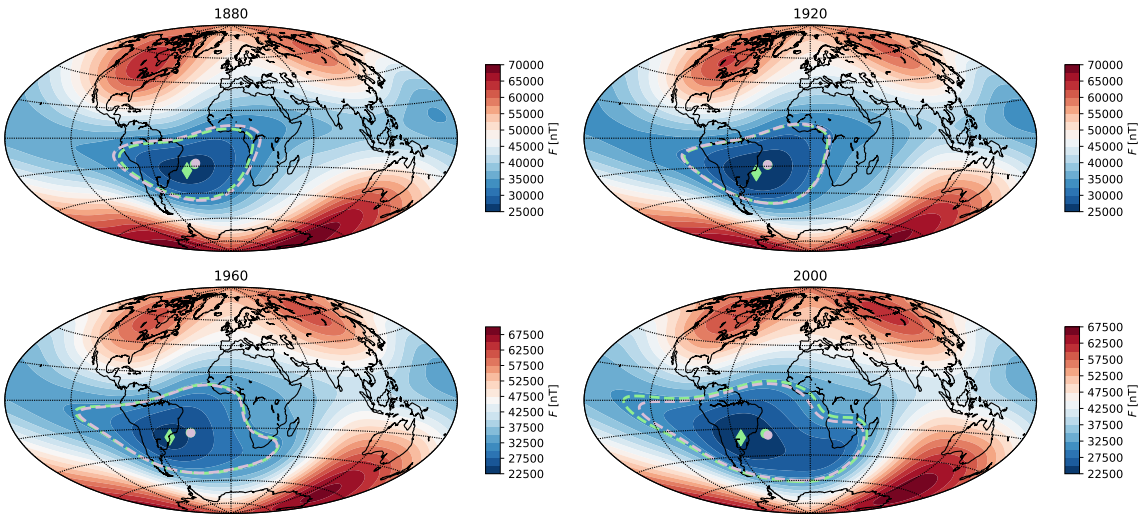

Fig. 3 Geomagnetic field intensity at Earth's surface for the mean model of COV-OBS.x1 at four snapshots (Gillet et al. 2015). Dashed green contours denote the *S*0 area, dashed purple contours denote the *S*1 area. Green diamonds denote the Min center, green and purple circles denote the centers of mass CM0 and CM1, respectively. Note the different scales from top to bottom

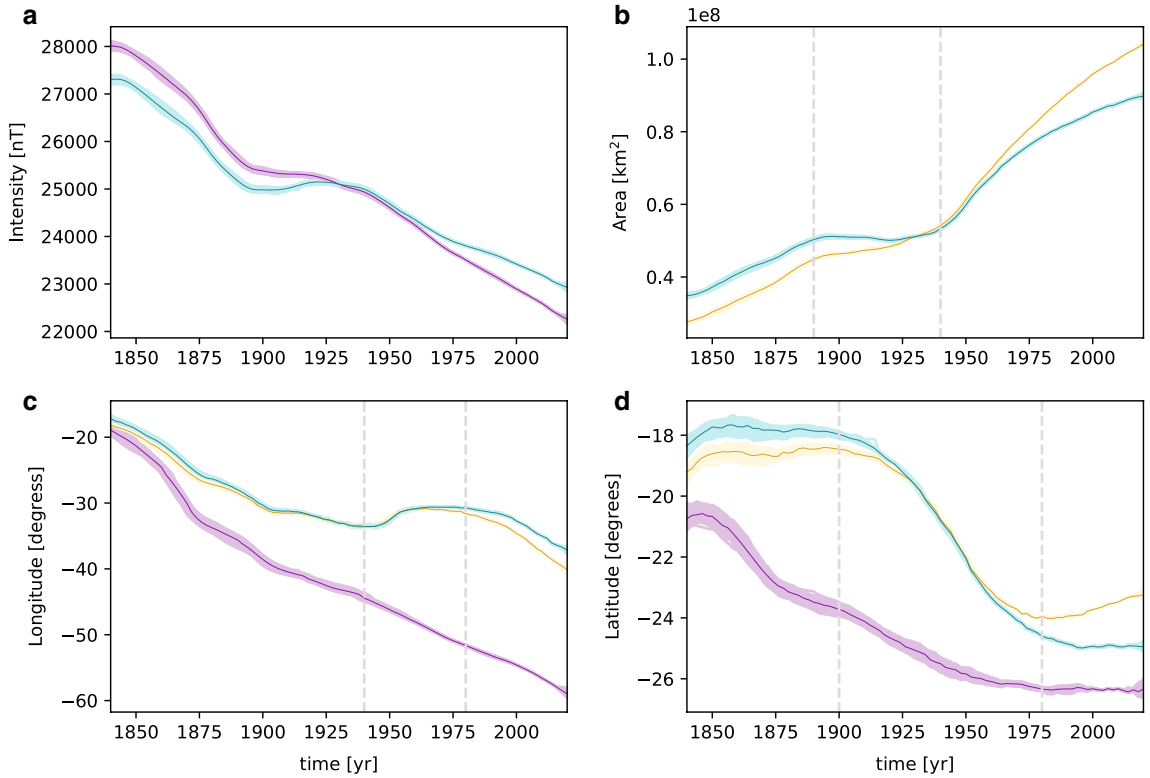

Fig. 4 SAA characterization vs. time for the period 1840–2020. Dark lines denote the mean model of COV-OBS.x1, light envelopes denote the 100 realizations of the ensemble. **a** Minimum intensity (purple) and the relative minimum intensity $|\vec{B}|^{\text{rel}}_{\text{min}}$ (turquoise). **b** Area based on *S*0 (yellow) and *S*1 (turquoise). **c** Longitude of center based on Min (purple), CM0 (yellow) and *CM*1 (turquoise). **d** Latitude of center based on Min (purple), CM0 (yellow) and CM1 (turquoise). Vertical dashed lines highlight special events of SAA area decrease (**b**), SAA center eastward drift (**c**) and SAA center rapid southward drift (**d**)

Table 1 Mean rates of change of the SAA area in 10^5 km^2/year and of the coordinates of its center in °/year for all models

Area	**1840–1890**	**1890–1940**	**1940–2020**	**Total**
*S*0	3.51	1.71	6.38	4.29
*S*1	3.18	0.27	4.56	2.98

Center longitude	**1840–1940**	**1940–1980**	**1980–2020**	**Total**
Min	−0.268	−0.189	−0.175	−0.229
CM0	−0.166	0.068	−0.226	−0.127
CM1	−0.177	0.087	−0.172	−0.117

Center co-latitude	**1840–1900**	**1900–1980**	**1980–2020**	**Total**
Min	0.059	0.034	0.000	0.035
CM0	−0.007	0.085	−0.021	0.031
CM1	0.000	0.096	0.007	0.044

Mean rates of change are given for specific periods motivated by Fig. 4 (see text) as well as for the entire period (denoted by 'Total')

in our preferred models *S*1 and CM1, the SAA area and motion are more non-linear including special events with distinctive trends.

Figure 4 also shows the results for the ensemble of all 100 realizations of COV-OBS.x1 (light colors). For all quantities, the envelopes around the mean values are

rather thin at all times, albeit slightly thicker at early periods. Clearly the SAA, being a surface property, is weakly sensitive to the small-scale field. We therefore conclude that the results in Fig. 4 are robust and insensitive to the field model realization.

Table 1 presents the mean rates of change of the SAA area and coordinates of center based on the various models. These mean rates of change correspond to the mean slopes of the corresponding quantities plotted in Fig. 4b–d. More specifically, in Table 1 we compare the mean rates of changes for the periods when the above mentioned special events were captured by our *S*1 and *CM*1 preferred models vs. the more 'typical' periods, i.e. when the SAA area increased and its center moved mostly westward with little latitudinal mobility. Our *S*1 model contains a period of ~ 50 years in which the SAA area was nearly flat. Moreover, the total rate of change of our *S*1 model is about 30% lower than that of the commonly used *S*0, demonstrating the contribution of the global surface intensity decrease to the apparent evolution of the SAA area based on the latter. The total westward drift of model Min is about twice larger than that of our *CM*1 model. In addition, according to *CM*1 the SAA drifted eastward during a period of ~ 40 years, whereas Min drifted westward throughout the entire period. Note that unlike the nearly flat SAA area decrease event of *S*1, the eastward drift event of *CM*1 is non-negligible, of about the same order of magnitude as its rate of westward drift over the entire period. Finally, according to model Min the SAA drifted southward monotonically and decelerated towards present day. In contrast, our model *CM*1 shows two periods with little latitudinal change and in between a period of ~ 80 years in which the SAA drifted southward in an impressive rate of 0.096°/year, nearly three times faster than the average southward drift rate of Min over the entire period.

We note that the mean rates reported in Table 1 should be considered with caution. Treating the SAA as a single point and a single area is somewhat artificial in the context of core dynamics. Indeed, as we will show in the next section, the temporal evolution of the SAA is affected by the motions of multiple geomagnetic flux patches on the CMB.

Outer core kinematic interpretation

What is the kinematic origin of the special events described above? Fig. 5 shows the radial geomagnetic field and its secular variation (SV) on the CMB. To infer features that are relevant for the large-scale surface field, both quantities are truncated at spherical harmonic degree and order 5 (see, e.g. Zossi et al. 2020). To analyze the special events captured by *S*1 and *CM*1, we examine three snapshots: 1920 during the SAA steady area and rapid southward drift; 1960 during the SAA eastward drift and (again) rapid southward drift; and 2000, a 'typical' reference snapshot. Although the non-linear intensity kernel is not centered right below the site, in practice the kernel is located around the surface observation site (Constable and Korte 2015; Terra-Nova et al. 2017; Panovska et al. 2019). We, therefore, centered the maps on the SAA region. For comparison, we also show the corresponding maps truncated at the maximum degree and order 14 of the field model (Fig. 6).

Our below interpretations of the SV of the SAA area and center are guided by the conclusions of Amit (2014): Correlation/anti-correlation between a radial field structure (or flux patch) with an SV structure indicates local intensification/weakening respectively, whereas coincidence of a flux patch with a center of a pair of opposite-sign SV structures suggests local drift. Following Terra-Nova et al. (2017), we focus on the main flux patches of both polarities below the SAA region. Synthetic tests demonstrate that weak surface field tends to reside near RFPs and away from NFPs (Terra-Nova et al. 2017, 2019).

The event of steady SAA area (based on *S*1) is related to the SV of the dominating RFPs on the CMB. In 1960 and 2000, the dominant RFP below south of Africa coincides with a same-sign SV structure (Fig. 5 middle and bottom), corresponding to local intensification, hence the 'typical' SAA area decrease. In contrast, in 1920, the dominant RFP below Patagonia coincides with a positive (i.e. opposite-sign) SV structure (Fig. 5, top), corresponding to local weakening, hence opposing the SAA area decrease and leading to the steady event.

The SAA eastward drift event (based on CM1) can be explained by the SV below mid-Atlantic between the Patagonia and Africa RFPs. In 1960 a southwest positive SV intrusion extends through mid-Atlantic until the southern tip of Patagonia (Fig. 5, middle), weakening the reversed flux below mid-atlantic. This period marks a transition between the dominant Patagonia RFP in the west Atlantic beforehand (Fig. 5, top) to the dominance of the Africa RFP in the east Atlantic later on (Fig. 5, bottom). The outcome of this transitional period is a brief eastward drift of the SAA.

The SAA rapid southward drift event (again based on *CM*1) is related to the SV of the high-latitude NFP below Antarctica during this period (Fig. 5, top and middle). In 1920 and 1960, this NFP drifted across Antarctica towards the Indian Ocean. Because this NFP is located south of the SAA, its drift away from the South Atlantic led to the rapid southward drift of the SAA. In contrast, in 2000 the SV below this NFP significantly faded (see SV scale in Fig. 5, bottom), resulting in the weak latitudinal motion of the SAA in 2000.

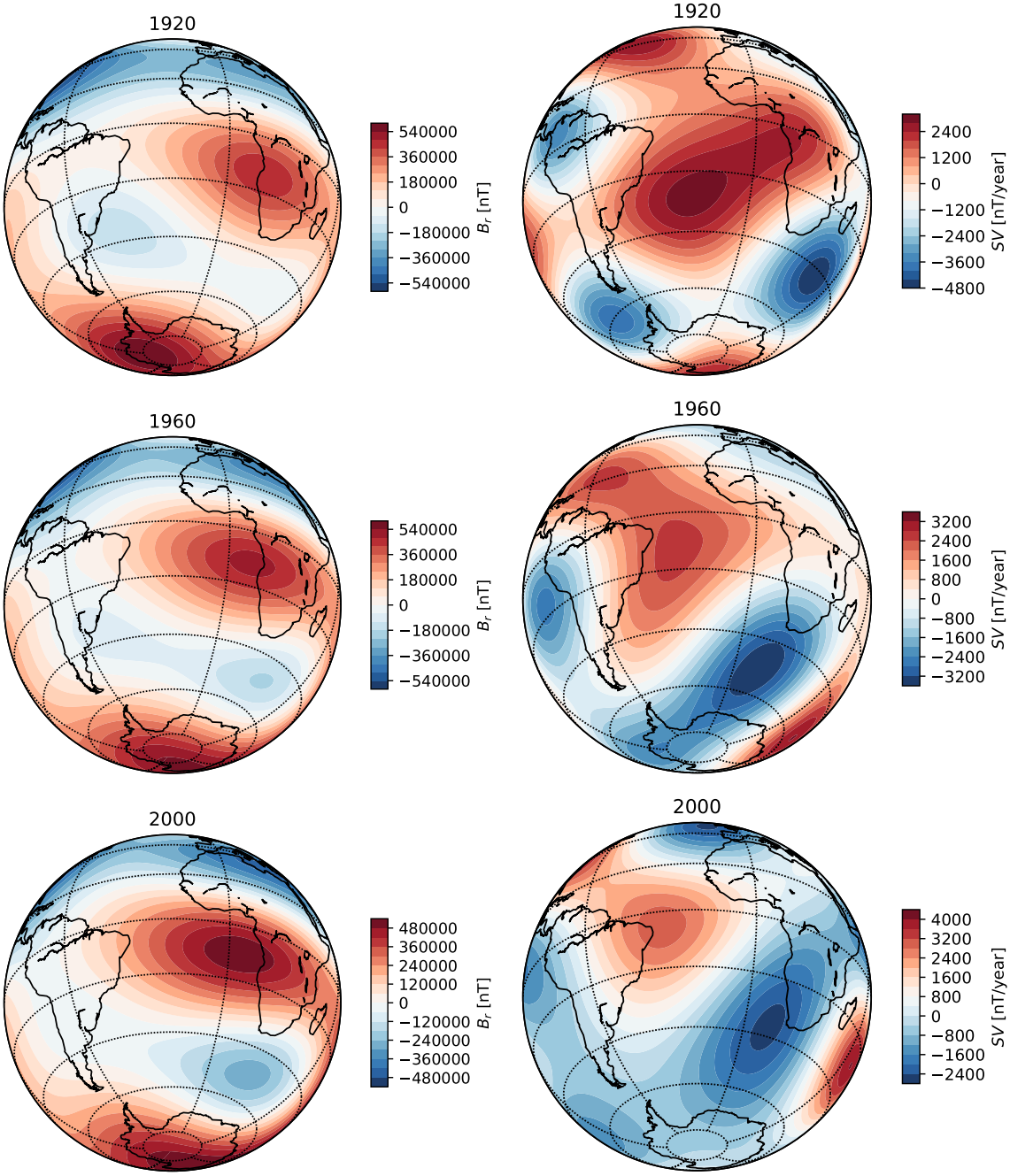

Fig. 5 Radial geomagnetic field (left) and its secular variation (right) at the core–mantle boundary for the mean model of COV-OBS.x1 in 1920 (top), 1960 (middle) and 2000 (bottom). All models are expanded until spherical harmonic degree and order 5. All maps are centered at 20°W 30°S, i.e. on the South Atlantic. Note the different scales

Finding the kinematic origins of the SAA SV in the more detailed maps expanded until spherical harmonic degree and order 14 (Fig. 6) is clearly more challenging. Nevertheless, some of the morphological relations between the radial field and its SV that we identified as the kinematic origins of the special SAA events based on the large-scale maps in Fig. 5 can also be detected in the small-scale counterpart maps in Fig. 6. These include the transition from a dominant RFP below Patagonia in 1920 (Figs. 5, 6, top) to the emergence of a dominant RFP below Africa (Figs. 5, 6, bottom). Another example is the dissipation of the NFP below Antarctica (Fig. 6) (see also Terra-Nova et al. 2017).

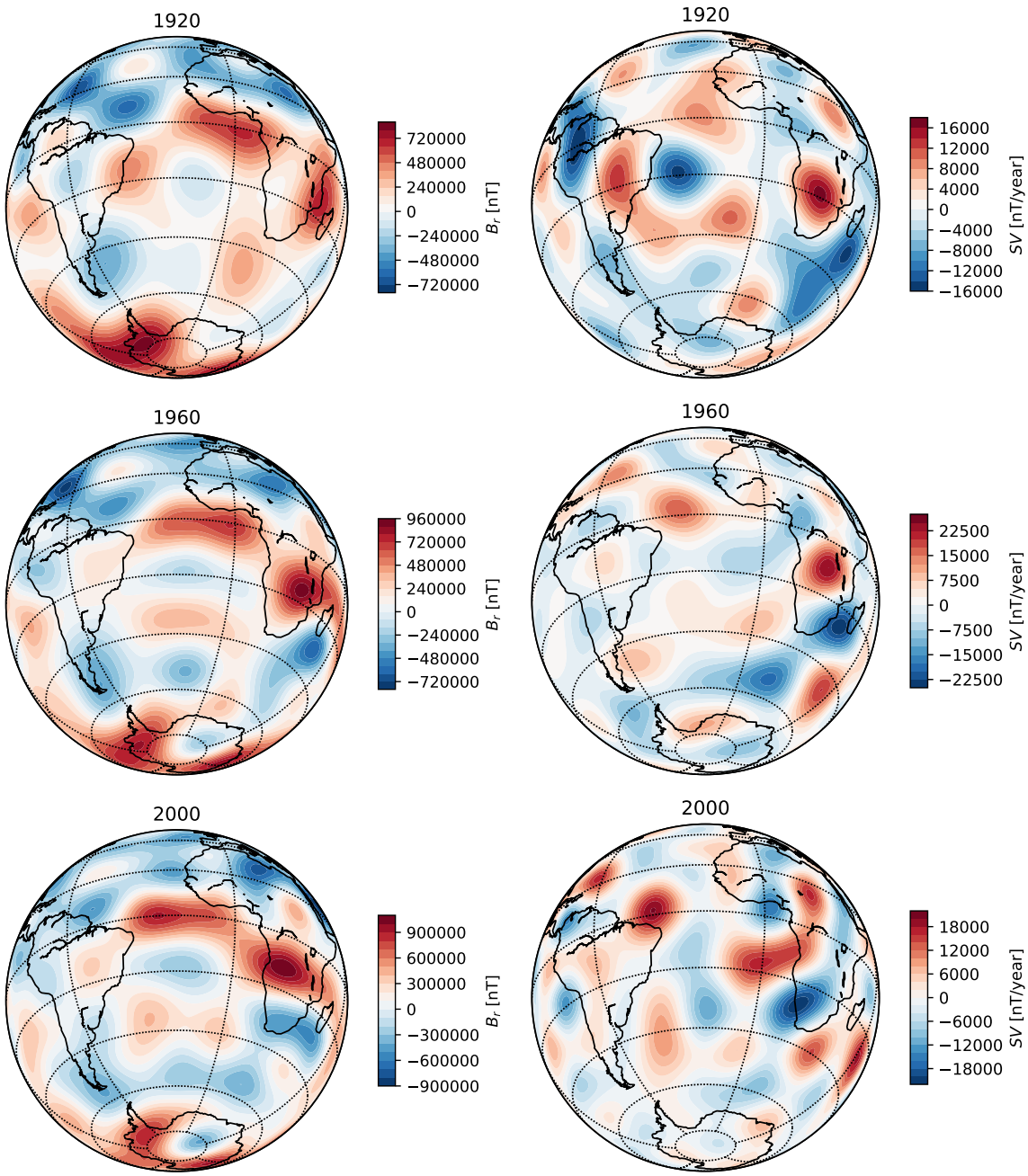

Fig. 6 As in Fig. 5 but expanded until spherical harmonic degree and order 14

There are two main differences between our interpretation of the SAA motion to that of Terra-Nova et al. (2017). First, we consider the *CM*1 model based on the center of mass of the area factored by the time-dependent mean surface intensity outside the SAA, whereas Terra-Nova et al. (2017) tracked the intensity minimum Min. Second, we analyzed the large-scale field and SV on the CMB which are in general appropriate for any surface application (Zossi et al. 2020), whereas Terra-Nova et al. (2017) explored the full field expanded until degree and order 14. Despite these differences, our results are in decent agreement with those of Terra-Nova et al. (2017), essentially pointing to the motions of the major RFPs and the high-latitude NFP below the South Atlantic region

as the dominating agents controlling the SAA motion, in particular its deviations from linearity.

Conclusions

We introduced simple new measures to characterize the SAA. Our area calculation accounts for temporal changes in the surface intensity away from the SAA, thus the resulting SAA area $S1$ isolates regional morphological variations. Our center calculation is regional (rather than local), thus the resulting SAA center $CM1$ integrates the effects of SAA anisotropy.

As in previous studies, we find that the SAA has overall been expanding and drifting westward and southward. However, we identified periods with exceptions to the SAA 'typical' area increase, westward drift and weak latitudinal change. These special events are non-detectable in the previous characterizations, highlighting the strongly time-dependent nature of the SAA. The special events and their kinematic origins are:

- 1890–1940: The SAA area was steady due to weakening of the Patagonia RFP.
- 1940–1980: The SAA center drifted eastward due to transition from early dominance of the RFP below Patagonia at its western limb to later dominance of the RFP below Africa at its eastern limb.
- 1900–1980: The SAA center drifted southward rapidly due to the drift of the high-latitude NFP below Antarctica away from the South Atlantic region.

It would be interesting to apply our characterization to archeomagnetic field models in order to find whether similar behavior persists over millennial timescales, bearing in mind the uncertainties in these field models (e.g. Constable and Korte 2015). This characterization may be used to constrain Earth-like numerical dynamos (Christensen et al. 2010; Davies and Constable 2014; Gastine et al. 2020), although these models operate in a non-realistic parameter space (e.g. Glatzmaier 2002). Continuous monitoring of Earth's geomagnetic field using surface observatories and dedicated satellite mission (such as the current Swarm constellation) will reveal whether the characterization obtained in this study persists in the future.

Abbreviations

SAA: South Atlantic Anomaly; RFP: Reversed flux patch; CMB: Core–mantle boundary; SV: Secular variation.

Acknowledgements

H. A. and M. L. thank Guy Moebs and Diana Saturnino for their help. We thank Javier Pavón-Carrasco and two anonymous reviewers for their important comments that improved the paper.

Authors' contributions

FT-N and ML produced the results. HA wrote the paper. All authors read and approved the final manuscript.

Funding

H. A. was supported by the Programme National de Plantologie (PNP) of CNRS/INSU, cofunded by CNES. F. T-N. acknowledges Sao Paulo Research Foundation (FAPESP) for Grant2018/07410-3.

Availability of data and materials

The geomagnetic field model COV-OBS.x1 analysed in this study is available in the followingweblink: http://www.spacecenter.dk/files/magnetic-models/COV-OBSx1/.

Competing interests

The authors declare that they have no competing interests.

Author details

[1] CNRS UMR 6112, Université de Nantes, Laboratoire de Planétologie et de Géodynamique, 2 rue de la Houssinière, Nantes 44000, France. [2] Departamento de Geofísica, Instituto de Astronomia, Geofísica e Ciências Atmosféricas, Universidade de São Paulo, Cidade Universitária, Rua do Matão, 1226, 05508-090 São Paulo, Brazil.

Received: 22 August 2020 Accepted: 9 January 2021
Published online: 08 February 2021

References

Amit H (2014) Can downwelling at the top of the Earth's core be detected in the geomagnetic secular variation? Phys Earth Planet Inter 229:110–121
Amit H, Aubert J, Hulot G (2010) Stationary, oscillating or drifting mantle-driven geomagnetic flux patches? J Geophys Res 115:B07108
Amit H, Choblet G, Olson P, Monteux J, Deschamps F, Langlais B, Tobie G (2015) Towards more realistic core-mantle boundary heat flux patterns: a source of diversity in planetary dynamos. Prog Earth Planet Sci 2:26. https://doi.org/10.1186/s40645-015-0056-3
Amit H, Korte M, Aubert J, Constable C, Hulot G (2011) The time-dependence of intense archeomagnetic flux patches. J Geophys Res 116:B12106
Anderson PC, Rich FJ, Borisov S (2018) Mapping the South Atlantic Anomaly continuously over 27 years. J Atmos Sol-Terr Phys 177:237–246
Aubert J (2015) Geomagnetic forecasts driven by thermal wind dynamics in the Earth's core. Geophys J Int 203:1738–1751
Aubert J, Amit H, Hulot G, Olson P (2008) Thermo-chemical wind flows couple Earth's inner core growth to mantle heterogeneity. Nature 454:758–761
Auvergne M, Bodin P, Boisnard L, Buey J-T, Chaintreuil S et al (2009) The CoRoT satellite in flight: description and performance. Astron Astrophys 506:411–424
Bloxham J, Gubbins D, Jackson A (1989) Geomagnetic secular variation. Phil Trans R Soc Lond A329:415–502
Brown M, Korte M, Holme R, Wardinski I, Gunnarson S (2018) Earth's magnetic field is (probably) not reversing. Proc Natl Acad Sci 115(20):5111–5116
Campuzano SA, Gómez-Paccard M, Pavón-Carrasco F, Osete ML (2019) Emergence and evolution of the South Atlantic Anomaly revealed by the new paleomagnetic reconstruction SHAWQ2k. Earth Planet. Sci. Lett. 512:17–26
Casadio S, Arino O (2011) Monitoring the South Atlantic Anomaly using ATSR instrument series. Adv Space Res 48(6):1056–1066
Christensen U, Aubert J, Hulot G (2010) Conditions for Earth-like geodynamo models. Earth Planets Sci Lett 296:487–496
Cnossen I, Maute A (2020) Simulated trends in ionosphere-thermosphere climate due to predicted main magnetic field changes from 2015 to 2065. J Geophys Res 125:e2019JA027738
Constable C, Korte M (2015) Centennial- to millennial-scale geomagnetic field variations. In: Kono M (ed) Treatise on geophysics, vol 5, 2nd edn. Elsevier Science, The Netherlands
Davies C, Constable C (2014) Insights from geodynamo simulations into long-term geomagnetic field behaviour. Earth Planets Sci Lett 404:238–249
De Santis A, Qamili E, Wu L (2013) Toward a possible next geomagnetic transition? Nat Hazards Earth Syst Sci 13:3395–3403

Deme S, Reitz G, Aapthy I, Hejja I, Lang E, Feher I (1999) Doses due to the South Atlantic Anomoly during the Euromir'95 mission measured by an on-board TLD system. Radiat Prot Dosim 85:301–304
Domingos J, Jault D, Pais MA, Mandea M (2017) The South Atlantic Anomaly throughout the solar cycle. Earth Planets Sci Lett 473:154–163
Dumberry M, More C (2020) Weak magnetic field changes over the Pacific due to high conductance in lowermost mantle. Nat Geosci 13:516–520
Finlay CC, Maus S, Beggan CD, Bondar TN, Chambodut A, Chernova TA, Chulliat A, Golovkov VP, Hamilton B, Hamoudi M, Holme R, Hulot G, Kuang W, Langlais B, Lesur V, Lowes FJ, Lühr H, Macmillan S, Mandea M, McLean S, Manoj C, Menvielle M, Michaelis I, Olsen N, Rauberg J, Rother M, Sabaka TJ, Tangborn A, Tøffner-Clausen L, Thébault E, Thomson AWP, Wardinski I, Wei Z, Zvereva TI (2010) International Geomagnetic Reference Field: the eleventh generation. Geophys J Int 183:1216–1230
Gastine T, Aubert J, Fournier A (2020) Dynamo-based limit to the extent of a stable layer atop Earth's core. Geophys J Int 222:1433-1448
Gillet N, Barrois O, Finlay CC (2015) Stochastic forecasting of the geomagnetic field from the COV-OBS.x1 geomagnetic field model, and candidate models for IGRF-12. Earth Planets Space 67:71. https://doi.org/10.1186/s40623-015-0225-z
Gillet N, Jault D, Finlay CC, Olsen N (2013) Stochastic modeling of the Earth's magnetic field: inversion for covariances over the observatory era. Geochem Geophys Geosyst 14:766–786. https://doi.org/10.1002/ggge.20041
Glatzmaier G (2002) Geodynamo simulations: how realistic are they? Annu Rev Earth Planets Sci Lett 30:237–257
Gubbins D, Willis P, Sreenivasan B (2007) Correlation of Earth's magnetic field with lower mantle thermal and seismic structure. Phys Earth Planet Inter 162:256–260
Hare V, Tarduno J, Huffman T, Watkeys M, Thebe P, Manyanga M, Bono R, Cottrell R (2018) New archeomagnetic directional records from Iron Age southern Africa (ca. 425–1550 CE) and implications for the South Atlantic Anomaly. Geophys Res Lett 45:1361–1369
Hartmann G, Pacca I (2009) Time evolution of the South Atlantic Magnetic Anomaly. An Acad Bras Cien 81:243–255
Hartmann GA, Poletti W, Trindade RIF, Ferreira LM (2019) New archeointensity data from South Brazil and the influence of the South Atlantic Anomaly in South America. Earth Planets Sci Lett 512:124–133
Heirtzler JR (2002) The future of the South Atlantic Anomaly and implications for radiation damage in space. J Atmos Solar Terr Phys 64:1701–1708
Hellio G, Gillet N (2018) Time-correlation-based regression of the geomagnetic field from archeological and sediment records. Geophys J Int 214(3):1585–1607
Jackson A, Jonkers A, Walker M (2000) Four centuries of geomagnetic secular variation from historical records. Phil Trans R Soc Lond A358:957–990
Konradi A, Badhwar GD, Braby LA (1994) Recent space shuttle observations of the South Atlantic Anomaly and radiation belt models. Adv Space Res 14:911–921
Lean J (2005) Living with a variable sun. Phys Today 58:32–38
Olson P, Amit H (2006) Changes in earth's dipole. Naturwissenschaften 93:519–542
Panovska S, Korte M, Constable CG (2019) One hundred thousand years of geomagnetic field evolution. Rev Geophys 57:1289–1337
Pavón-Carrasco F, De Santis A (2016) The South Atlantic Anomaly: the key for a possible geomagnetic reversal. Front Earth Sci 4:40. https://doi.org/10.3389/feart.2016.00040
Schaefer RK, Paxton LJ, Selby C, Ogorzalek B, Romeo G, Wolven B, Hsieh S (2016) Observation and modeling of the South Atlantic Anomaly in low Earth orbit using photometric instrument data. Space Weather 14:330–342
Tarduno J, Watkeys M, Huffman T, Cottrell D, Blackman E, Wendt A, Scribner A, Wagner C (2015) Antiquity of the South Atantic Anomaly and evidence for top-down control on the geodynamo. Nat. Commun. 6:7865. https://doi.org/10.1038/ncomms8865
Tarduno JA (2018) Subterranean clues to the future of our planetary magnetic shield. Proc Nat Acad Sci 115:13154–13156
Terra-Nova F, Amit H, Choblet G (2019) Preferred locations of weak surface field in numerical dynamos with heterogeneous core-mantle boundary heat flux: consequences for the South Atlantic Anomaly. Geophys J Int 217:1179–1199
Terra-Nova F, Amit H, Hartmann GA, Trindade RIF, Pinheiro KJ (2017) Relating the South Atlantic Anomaly and geomagnetic flux patches. Phys Earth Planet Inter 266:39–53
Trindade R, Jaqueto P, Terra-Nova F, Brandt D, Hartmann GA, Feinberg J, Strauss BE, Novello VF, Cruz FW, Karmann I, Cheng H, Edwards RL (2018) Speleothem record of geomagnetic South Atlantic Anomaly recurrence. Proc Nat Acad Sci 115:13198–13203
Zossi B, Fagre M, Amit H, Elias AG (2020) Geomagnetic field model indicates shrinking northern auroral oval. J Geophys Res 125:e2019JA027434

Publisher's Note